Size-dependent correlation effects in the ultrafast optical dynamics of metal nanoparticles

T. V. Shahbazyan and I. E. Perakis
Department of Physics and Astronomy, Vanderbilt University, Box 1807-B, Nashville, Tennessee 37235
(Received 1 February 1999; revised manuscript received 20 April 1999)

We study the role of collective surface excitations in electron relaxation in small metal particles. We show that dynamically screened electron-electron interaction in a nanoparticle contains a size-dependent correction induced by the surface. This leads to channels of quasiparticle scattering accompanied by the emission of surface collective excitations. We calculate the energy and temperature dependence of the corresponding rates, which depend strongly on the nanoparticle size. We show that the surface-plasmon-mediated scattering rate of a conduction electron increases with energy, in contrast to that mediated by a bulk plasmon. In noble-metal particles, we find that the dipole collective excitations (surface plasmons) mediate a resonant scattering of *d* holes to the conduction band. We show that, with decreasing nanoparticle size, the latter effect leads to a strong frequency dependence of the relaxation near the surface-plasmon resonance, while for even smaller sizes of a few nanometers we predict a drastic change in the differential absorption line shape. The experimental implications of our results in ultrafast spectroscopy are discussed. [S0163-1829(99)08935-3]

I. INTRODUCTION

The properties of small metal particles in the intermediate regime between bulklike and molecular behavior have been a subject of great interest recently.[1–5] Even though the electronic and optical properties of nanoparticles have been extensively studied, the role of confinement in the electron dynamics is much less understood. Examples of outstanding issues include the role of electron-electron interactions in the process of cluster fragmentation, the role of surface lattice modes in providing additional channels for intramolecular energy relaxation, the influence of the electron and nuclear motion on the superparamagnetic properties of clusters, and the effect of confinement on the nonlinear optical properties and transient response under ultrafast excitation.[1,2,4,5] These and other time-dependent phenomena can be studied with femtosecond nonlinear optical spectroscopy, which allows one to probe the dynamics of the excited states on time scales shorter than the energy relaxation or the polarization dephasing times.

Surface collective excitations play an important role in the absorption of light by metal nanoparticles. In large particles with sizes comparable to the wavelength of light λ (but smaller than the bulk mean free path), the line shape of the surface-plasmon (SP) resonance is determined by the electromagnetic effects.[1] On the other hand, in small nanoparticles with radii $R \ll \lambda$, the absorption spectrum is governed by quantum confinement effects. For example, the momentum nonconservation due to the confining potential leads to a Landau damping of the SP and to a resonance linewidth inversely proportional to the nanoparticle size.[1,6] The nonlinear optical properties of small nanoparticles are also affected by the confinement: a size-dependent enhancement of the third-order susceptibilities, caused by the elastic surface scattering of single-particle excitations, has been reported.[7–9]

Extensive experimental studies of the electron relaxation in nanoparticles have recently been performed using ultrafast pump-probe spectroscopy.[10–17] Unlike in semiconductors, the dephasing processes in metals are very fast, and nonequilibrium populations of optically excited electrons and holes are formed within several femtoseconds. These thermalize into the hot Fermi-Dirac distribution within several hundreds of femtoseconds, mainly due to *e*-*e* and *h*-*h* scattering.[18–21] Since the electron heat capacity is much smaller than that of the lattice, a high electron temperature can be reached during subpicosecond time scales, i.e., before any significant energy transfer to the phonon bath occurs. During this stage, the SP resonance was observed to undergo a time–dependent spectral broadening.[10,12,14] Subsequently, the electron and phonon baths equilibrate through the electron-phonon interactions over time intervals of a few picoseconds. During this incoherent stage, the hot-electron distribution can be characterized by a time-dependent temperature. Correlation effects play an important role in the latter regime. For example, in order to explain the differential absorption line shape, it is essential to take into account the *e*-*e* scattering of the optically excited carriers near the Fermi surface.[12] Furthermore, despite the similarities to the bulklike behavior, observed, e.g., in metal films, certain aspects of the optical dynamics in nanoparticles are significantly different.[15,12,17] For example, experimental studies of small Cu nanoparticles revealed that the relaxation times of the pump-probe signal depend strongly on frequency: the relaxation was considerably slower at the SP resonance.[12,17] These and other observations suggest that collective surface excitations play an important role in the electron dynamics in small metal particles.

Let us recall the basic facts regarding the linear absorption by metal nanoparticles embedded in a medium with dielectric constant ϵ_m. We will focus primarily on noble-metal particles containing several hundred atoms; in this case, the confinement affects the extended electronic states even though the bulk lattice structure has been established. When the particle radii are small, $R \ll \lambda$, so that only dipole surface modes can be optically excited and nonlocal effects can be neglected, the optical properties of this system are determined by the dielectric function[1]

$$\epsilon_{\rm col}(\omega) = \epsilon_m + 3p\,\epsilon_m \frac{\epsilon(\omega) - \epsilon_m}{\epsilon(\omega) + 2\epsilon_m}, \tag{1}$$

where $\epsilon(\omega)=\epsilon'(\omega)+i\epsilon''(\omega)$ is the dielectric function of a metal particle and $p\ll 1$ is the volume fraction occupied by nanoparticles in the colloid. Since the *d* electrons play an important role in the optical properties of noble metals, the dielectric function $\epsilon(\omega)$ also includes the interband contribution $\epsilon_d(\omega)$. For $p\ll 1$, the absorption coefficient of such a system is proportional to that of a single particle, and is given by[1]

$$\alpha(\omega)=-9p\epsilon_m^{3/2}\frac{\omega}{c}\mathrm{Im}\frac{1}{\epsilon_s(\omega)}, \tag{2}$$

where

$$\epsilon_s(\omega)=\epsilon_d(\omega)-\omega_p^2/\omega(\omega+i\gamma_s)+2\epsilon_m \tag{3}$$

plays the role of an effective dielectric function of a particle in the medium. Its zero, $\epsilon_s'(\omega_s)=0$, determines the frequency of the SP, ω_s. In Eq. (3), ω_p is the bulk plasmon frequency of the conduction electrons, and the width γ_s characterizes the SP damping. The semiclassical result [Eqs. (2) and (3)] applies to nanoparticles with radii $R\gg q_{\mathrm{TF}}^{-1}$, where q_{TF} is the Thomas-Fermi screening wave vector ($q_{\mathrm{TF}}^{-1}\sim 1$ Å in noble metals). In this case, the electron density deviates from its classical shape only within a surface layer occupying a small fraction of the total volume.[22] Quantum-mechanical corrections, arising from the discrete energy spectrum, lead to a width $\gamma_s\sim v_F/R$, where $v_F=k_F/m$ is the Fermi velocity[1,6] (we set $\hbar=1$ throughout the paper). Even though $\gamma_s/\omega_s\sim(q_{\mathrm{TF}}R)^{-1}\ll 1$, this damping mechanism dominates over others, e.g., due to phonons, for sizes $R\lesssim 10$ nm. On the other hand, in small clusters containing several dozen atoms, this semiclassical approximation breaks down and density functional or *ab initio* methods should be used.[1–4]

It should be noted that, in contrast to the surface collective excitations, the *e-e* scattering is not sensitive to the nanoparticle size as long as the condition $q_{\mathrm{TF}}R\gg 1$ holds.[23] Indeed, for such sizes, the static screening is essentially bulklike. At the same time, the energy dependence of the bulk *e-e* scattering rate,[24] $\gamma_e\propto(E-E_F)^2$, with E_F being the Fermi energy, comes from the phase-space restriction due to the momentum conservation, and involves the exchange of typical momenta $q\sim q_{\mathrm{TF}}$. If the size-induced momentum uncertainty $\delta q\sim R^{-1}$ is much smaller than q_{TF}, the *e-e* scattering rate in a nanoparticle is not significantly affected by the confinement.[25]

In this paper we study the role of collective surface excitations in the dynamical response of metal nanoparticles. We provide a detailed account of our preliminary results published earlier,[17] and present results on the size dependence of the ultrafast dynamics in small metal particles. In particular, we derive an explicit expression for the dynamically screened *e-e* interaction, and show that it contains a size-dependent correction originating from the surface collective modes excited by an electron inside the nanoparticle. This opens up quasiparticle scattering channels mediated by surface collective modes. We then describe the effect of such collective surface excitations on the scattering rate of the Fermi sea conduction electrons. We show that the latter increases with energy, in contrast to the bulk-plasmon-mediated scattering, and, with decreasing size, leads to a series of steps at the surface collective excitation energies on top of the smooth background of the bulklike scattering rate. We also study the size dependence of the differential absorption line shape, and show that, in noble-metal particles, it should undergo a dramatic transformation, from the apparent SP redshift[17] to an apparent SP blueshift with decreasing size. This prediction points out the important role of the correlations between single-particle and collective surface excitations on the ultrafast pump-probe dynamics before the onset of the transition from metal to insulator (the molecular cluster regime where discrete level quantization prevails). We also show that the relaxation times of the pump-probe signal depend strongly on the probe frequency, and describe the changes in such a frequency dependence as the nanoparticle size decreases.

The paper is organized as follows. In Sec. II we derive the dynamically screened Coulomb potential in a nanoparticle. In Sec. III we calculate the SP-mediated quasiparticle scattering rates of the conduction electrons and the *d*-band holes. In Sec. IV we incorporate these effects into the calculation of the absorption spectrum and study their role in the size and frequency dependence of the time-resolved pump-probe signal.

II. ELECTRON-ELECTRON INTERACTIONS IN METAL NANOPARTICLES

In this section, we study the effect of the surface collective excitations on the *e-e* interactions in a spherical metal particle. We present the detailed derivation of the dynamically screened Coulomb potential,[17] by generalizing a method previously developed for calculations of local-field corrections to the optical fields.[26]

The potential $U(\omega;\mathbf{r},\mathbf{r}')$ at point $\mathbf{r}$ arising from an electron at point $\mathbf{r}'$ is determined by the equation[27]

$$U(\omega;\mathbf{r},\mathbf{r}')=u(\mathbf{r}-\mathbf{r}')+\int d\mathbf{r}_1 d\mathbf{r}_2 u(\mathbf{r}-\mathbf{r}_1)\times\Pi(\omega;\mathbf{r}_1,\mathbf{r}_2)U(\omega;\mathbf{r}_2,\mathbf{r}'), \tag{4}$$

where $u(\mathbf{r}-\mathbf{r}')=e^2|\mathbf{r}-\mathbf{r}'|^{-1}$ is the unscreened Coulomb potential and $\Pi(\omega;\mathbf{r}_1,\mathbf{r}_2)$ is the polarization operator. There are three contributions to Π, arising from the polarization of the conduction electrons, the *d* electrons, and the medium surrounding the nanoparticles: $\Pi=\Pi_c+\Pi_d+\Pi_m$. It is useful to rewrite Eq. (4) in the ''classical'' form

$$\nabla\cdot(\mathbf{E}+4\pi\mathbf{P})=4\pi e^2\delta(\mathbf{r}-\mathbf{r}'), \tag{5}$$

where $\mathbf{E}(\omega;\mathbf{r},\mathbf{r}')=-\nabla U(\omega;\mathbf{r},\mathbf{r}')$ is the screened Coulomb field and $\mathbf{P}=\mathbf{P}_c+\mathbf{P}_d+\mathbf{P}_m$ is the electric polarization vector, related to the potential *U* as

$$\nabla\mathbf{P}(\omega;\mathbf{r},\mathbf{r}')=-e^2\int d\mathbf{r}_1\Pi(\omega;\mathbf{r},\mathbf{r}_1)U(\omega;\mathbf{r}_1,\mathbf{r}'). \tag{6}$$

In the random-phase approximation (RPA), the intraband polarization operator is given by

$$\Pi_c(\omega;\mathbf{r},\mathbf{r}')=\sum_{\alpha\alpha'}\frac{f(E^c_\alpha)-f(E^c_{\alpha'})}{E^c_\alpha-E^c_{\alpha'}+\omega+i0}\times\psi^c_\alpha(\mathbf{r})\psi^{c*}_{\alpha'}(\mathbf{r})\psi^{c*}_\alpha(\mathbf{r}')\psi^c_{\alpha'}(\mathbf{r}'),\qquad(7)$$

where E^c_α and ψ^c_α are the single-electron eigenenergies and eigenfunctions in the nanoparticle, and $f(E)$ is the Fermi-Dirac distribution (we set $\hbar=1$). Since we are interested in frequencies much larger than the single-particle level spacing, $\Pi_c(\omega)$ can be expanded in terms of $1/\omega$. For the real part $\Pi'_c(\omega)$, in the leading order we obtain

$$\Pi'_c(\omega;\mathbf{r},\mathbf{r}_1)=-\frac{1}{m\omega^2}\nabla[n_c(\mathbf{r})\nabla\delta(\mathbf{r}-\mathbf{r}_1)],\qquad(8)$$

where $n_c(\mathbf{r})$ is the conduction electron density. In the following we assume, for simplicity, a step density profile, $n_c(\mathbf{r})=\overline{n_c}\,\theta(R-r)$, where $\overline{n_c}$ is the average density. The leading contribution to the imaginary part, $\Pi''_c(\omega)$, is proportional to ω^{-3}, so that $\Pi''_c(\omega)\ll\Pi'_c(\omega)$.

By using Eqs. (8) and (6), we obtain a familiar expression for $\mathbf{P}_c$ at high frequencies,

$$\mathbf{P}_c(\omega;\mathbf{r},\mathbf{r}')=\frac{e^2n_c(\mathbf{r})}{m\omega^2}\nabla U(\omega;\mathbf{r},\mathbf{r}')=\theta(R-r)\chi_c(\omega)\mathbf{E}(\omega;\mathbf{r},\mathbf{r}'),\qquad(9)$$

where $\chi_c(\omega)=-e^2\overline{n_c}/m\omega^2$ is the conduction electron susceptibility. Note that, for a step density profile, $\mathbf{P}_c$ vanishes outside the particle. The d-band and dielectric medium contributions to $\mathbf{P}$ are also given by similar relations,

$$\mathbf{P}_d(\omega;\mathbf{r},\mathbf{r}')=\theta(R-r)\chi_d(\omega)\mathbf{E}(\omega;\mathbf{r},\mathbf{r}'),\qquad(10)$$

$$\mathbf{P}_m(\omega;\mathbf{r},\mathbf{r}')=\theta(r-R)\chi_m\mathbf{E}(\omega;\mathbf{r},\mathbf{r}'),\qquad(11)$$

where $\chi_i=(\epsilon_i-1)/4\pi$, $i=d,m$ are the corresponding susceptibilities, and the step functions account for the boundary conditions.[28] Using Eqs. (9)–(11), one can write a closed-form equation for $U(\omega;\mathbf{r},\mathbf{r}')$. Using Eq. (6), the second term of Eq. (4) can be presented as $-e^{-2}\int d\mathbf{r}_1u(\mathbf{r}-\mathbf{r}_1)\nabla\cdot\mathbf{P}(\omega;\mathbf{r}_1,\mathbf{r}')$. Substituting the above expressions for $\mathbf{P}$, we then obtain, after integrating by parts,

$$\epsilon(\omega)U(\omega;\mathbf{r},\mathbf{r}')=\frac{e^2}{|\mathbf{r}-\mathbf{r}'|}+\int d\mathbf{r}_1\nabla_1\frac{1}{|\mathbf{r}-\mathbf{r}_1|}\cdot\nabla_1[\theta(R-r)\times\chi(\omega)+\theta(r-R)\chi_m]U(\omega;\mathbf{r}_1,\mathbf{r}')+i\int d\mathbf{r}_1d\mathbf{r}_2\frac{e^2}{|\mathbf{r}-\mathbf{r}_1|}\times\Pi''_c(\omega;\mathbf{r}_1,\mathbf{r}_2)U(\omega;\mathbf{r}_2,\mathbf{r}'),\qquad(12)$$

with

$$\epsilon(\omega)\equiv1+4\pi\chi(\omega)=\epsilon_d(\omega)-\omega_p^2/\omega^2,\qquad(13)$$

$\omega_p^2=4\pi e^2\overline{n_c}/m$ being the plasmon frequency in the conduction band. The last term on the right-hand side of Eq. (12), proportional to $\Pi''_c(\omega)$, can be regarded as a small correction. To solve Eq. (12), we first eliminate the angular dependence by expanding $U(\omega;\mathbf{r},\mathbf{r}')$ in spherical harmonics, $Y_{LM}(\hat{\mathbf{r}})$, with coefficients $U_{LM}(\omega;r,r')$. Using the corresponding expansion of $|\mathbf{r}-\mathbf{r}'|^{-1}$ with coefficients $Q_{LM}(r,r')=[4\pi/(2L+1)]r^{-L-1}r'^L$ (for $r>r'$), we obtain the following equation for $U_{LM}(\omega;r,r')$:

$$\epsilon(\omega)U_{LM}(\omega;r,r')=Q_{LM}(r,r')+4\pi[\chi(\omega)-\chi_m]\frac{L+1}{2L+1}\left(\frac{r}{R}\right)^LU_{LM}(\omega;R,r')+ie^2\sum_{L'M'}\int dr_1dr_2r_1^2r_2^2Q_{LM}(r,r_1)\Pi''_{LM,L'M'}(\omega;r_1,r_2)U_{L'M'}(\omega;r_2,r'),\qquad(14)$$

where

$$\Pi''_{LM,L'M'}(\omega;r_1,r_2)=\int d\hat{\mathbf{r}}_1d\hat{\mathbf{r}}_2Y^*_{LM}(\hat{\mathbf{r}}_1)\Pi''_c(\omega;\mathbf{r}_1,\mathbf{r}_2)Y_{L'M'}(\hat{\mathbf{r}}_2)\qquad(15)$$

are the coefficients of the multipole expansion of $\Pi''_c(\omega;\mathbf{r}_1,\mathbf{r}_2)$. For $\Pi''_c=0$, the solution of Eq. (14) can be presented in the form

$$U_{LM}(\omega;r,r')=a(\omega)e^2Q_{LM}(r,r')+b(\omega)\frac{4\pi e^2}{2L+1}\frac{r^Lr'^L}{R^{2L+1}},\qquad(16)$$

with frequency-dependent coefficients a and b. Since $\Pi''_c(\omega)\ll\Pi'_c(\omega)$ for the relevant frequencies, the solution of Eq. (14) in the presence of the last term can be written in the same form as Eq. (16), but with modified $a(\omega)$ and $b(\omega)$. Substituting Eq. (16) into Eq. (14), after lengthy algebra we obtain in the lowest order in Π''_c,

$$a(\omega)=\epsilon^{-1}(\omega),\quad b(\omega)=\epsilon_L^{-1}(\omega)-\epsilon^{-1}(\omega),\qquad(17)$$

where

$$\epsilon_L(\omega)=\frac{L}{2L+1}\epsilon(\omega)+\frac{L+1}{2L+1}\epsilon_m+i\epsilon''_{cL}(\omega)\qquad(18)$$

is the effective dielectric function, whose zero, $\epsilon'_L(\omega_L)=0$, determines the frequency of the collective surface excitation with angular momentum L,[1]

$$\omega_L^2=\frac{L\omega_p^2}{L\epsilon_d'(\omega_L)+(L+1)\epsilon_m}. \tag{19}$$

In Eq. (18), $\epsilon_{cL}''(\omega)$ characterizes the damping of the L-pole collective mode by single-particle excitations, and is given by

$$\epsilon_{cL}''(\omega)=\frac{4\pi^2e^2}{(2L+1)R^{2L+1}}\sum_{\alpha\alpha'}|M_{\alpha\alpha'}^{LM}|^2[f(E_\alpha^c)-f(E_{\alpha'}^c)]\times\delta(E_\alpha^c-E_{\alpha'}^c+\omega), \tag{20}$$

where $M_{\alpha\alpha'}^{LM}$ are the matrix elements of $r^LY_{LM}(\hat{\mathbf{r}})$. Due to the momentum nonconservation in a nanoparticle, the matrix elements are finite, which leads to the size-dependent width of the L-pole mode:[6,26]

$$\gamma_L=\frac{2L+1}{L}\frac{\omega^3}{\omega_p^2}\epsilon_{cL}''(\omega). \tag{21}$$

For $\omega\sim\omega_L$, one can show that the width $\gamma_L\sim v_F/R$ is independent of ω. Note that, in noble-metal particles, there is an additional d-electron contribution to the imaginary part of $\epsilon_L(\omega)$ at frequencies above the onset Δ of the interband transitions.

Putting everything together, we arrive at the following expression for the dynamically-screened interaction potential in a nanoparticle:

$$U(\omega;\mathbf{r},\mathbf{r}')=\frac{u(\mathbf{r}-\mathbf{r}')}{\epsilon(\omega)}+\frac{e^2}{R}\times\sum_{LM}\frac{4\pi}{2L+1}\frac{1}{\tilde{\epsilon}_L(\omega)}\left(\frac{rr'}{R^2}\right)^L Y_{LM}(\hat{\mathbf{r}})Y_{LM}^*(\hat{\mathbf{r}}'), \tag{22}$$

with $\tilde{\epsilon}_L^{-1}(\omega)=\epsilon_L^{-1}(\omega)-\epsilon^{-1}(\omega)$. Equation (22), which is the main result of this section, represents a generalization of the plasmon-pole approximation to spherical particles. The two contributions to the rhs originate from two types of dynamical screening. The first describes the usual bulklike screening of the Coulomb potential by the electrons inside the particle. The second contribution is an effective interaction induced by the *surface*: the potential of an electron inside the nanoparticle excites high-frequency surface collective modes, which in turn act as image charges that interact with the second electron. It should be emphasized that, unlike in the case of the optical fields, the surface-induced dynamical screening of the Coulomb potential is *size dependent*.

Note that the excitation energies of the surface collective modes are lower than the bulk-plasmon energy, also given by Eq. (19) but with $\epsilon_m=0$. This opens up new channels of quasiparticle scattering, considered in Sec. III.

III. QUASIPARTICLE SCATTERING VIA SURFACE COLLECTIVE MODES

A. Conduction electron scattering

In this subsection, we calculate the rates of electron scattering in the conduction band accompanied by the emission of surface collective modes, and discuss its possible experimental manifestations. In the first order in the surface-induced potential, given by the second term on the right-hand side of Eq. (22), the corresponding scattering rate can be obtained from the Matsubara self-energy:[27]

$$\Sigma_\alpha^c(i\omega)=-\frac{1}{\beta}\sum_{i\omega'}\sum_{LM}\sum_{\alpha'}\frac{4\pi e^2}{(2L+1)R^{2L+1}}\frac{|M_{\alpha\alpha'}^{LM}|^2}{\tilde{\epsilon}_L(i\omega')}\times G_{\alpha'}^c(i\omega'+i\omega), \tag{23}$$

where $G_\alpha^c=(i\omega-E_\alpha^c)^{-1}$ is the noninteracting Green function of the conduction electron. Here the matrix elements $M_{\alpha\alpha'}^{LM}$ are calculated with the one-electron wave functions $\psi_\alpha^c(\mathbf{r})=R_{nl}(r)Y_{lm}(\hat{\mathbf{r}})$. Since $|\alpha\rangle$ and $|\alpha'\rangle$ are the initial and final states of the scattered electron, the main contribution to the Lth term of the angular momentum sum in Eq. (23) will come from electron states with energy difference $E_\alpha-E_{\alpha'}\sim\omega_L$. Therefore, $M_{\alpha\alpha'}^{LM}$ can be expanded in terms of the small parameter $E_0/|E_\alpha^c-E_{\alpha'}^c|\sim E_0/\omega_L$, where $E_0=(2mR^2)^{-1}$ is the characteristic confinement energy. The leading term can be obtained by using the following procedure.[6,26] We present $M_{\alpha\alpha'}^{LM}$ as

$$M_{\alpha\alpha'}^{LM}=\langle c,\alpha|r^LY_{LM}(\hat{\mathbf{r}})|c,\alpha'\rangle=\frac{\langle c,\alpha|[H,[H,r^LY_{LM}(\hat{\mathbf{r}})]]|c,\alpha'\rangle}{(E_\alpha^c-E_{\alpha'}^c)^2}, \tag{24}$$

where $H=H_0+V(r)$ is the Hamiltonian of an electron in a nanoparticle with confining potential $V(r)=V_0\theta(r-R)$. Since $[H,r^LY_{LM}(\hat{\mathbf{r}})]=-(1/m)\nabla[r^LY_{LM}(\hat{\mathbf{r}})]\cdot\nabla$, the numerator in Eq. (24) contains a term proportional to the gradient of the confining potential, which peaks sharply at the surface. The corresponding contribution to the matrix element describes the surface scattering of an electron making the L-pole transition between the states $|c,\alpha\rangle$ and $|c,\alpha'\rangle$, and gives the dominant term of the expansion. Thus, in leading order in $|E_\alpha^c-E_{\alpha'}^c|^{-1}$, we obtain

$$M_{\alpha\alpha'}^{LM}=\frac{\langle c,\alpha|\nabla[r^LY_{LM}(\hat{\mathbf{r}})]\cdot\nabla V(r)|c,\alpha'\rangle}{m(E_\alpha^c-E_{\alpha'}^c)^2}=\frac{LR^{L+1}}{m(E_\alpha^c-E_{\alpha'}^c)^2}V_0R_{nl}(R)R_{n'l'}(R)\varphi_{lm,l'm'}^{LM}, \tag{25}$$

with $\varphi_{lm,l'm'}^{LM}=\int d\hat{\mathbf{r}}Y_{lm}^*(\hat{\mathbf{r}})Y_{LM}(\hat{\mathbf{r}})Y_{l'm'}(\hat{\mathbf{r}})$. Note that, for $L=1$, Eq. (25) becomes exact. For electron energies close to the Fermi level, $E_{nl}^c\sim E_F$, the radial quantum numbers are large, and the product $V_0R_{nl}(R)R_{n'l'}(R)$ can be evaluated by using semiclassical wave functions. In the limit $V_0\to\infty$,

this product is given by[6] $2\sqrt{E^c_{nl}E^c_{n'l'}}/R^3$, where $E^c_{nl}=\pi^2(n+l/2)^2E_0$ is the electron eigenenergy for large n. Substituting this expression into Eq. (25) and then into Eq. (23), we obtain

$$\Sigma^c_\alpha(i\omega)=-\frac{1}{\beta}\sum_{i\omega'}\sum_{L}\sum_{n'l'}C^L_{ll'}\times\frac{4\pi e^2}{(2L+1)R}\frac{E^c_{nl}E^c_{n'l'}}{(E^c_{nl}-E^c_{n'l'})^4}\frac{(4LE_0)^2}{\tilde{\epsilon}_L(i\omega')}\times G^c_{\alpha'}(i\omega'+i\omega), \tag{26}$$

with

$$C^L_{ll'}=\sum_{M,m'}|\varphi^{LM}_{lm,l'm'}|^2=\frac{(2L+1)(2l'+1)}{8\pi}\int_{-1}^{1}dxP_l(x)P_L(x)P_{l'}(x), \tag{27}$$

where $P_l(x)$ are Legendre polynomials; we used properties of the spherical harmonics in the derivation of Eq. (27). For $E^c_{nl}\sim E_F$, the typical angular momenta are large, $l\sim k_FR\gg 1$, and one can use the large-l asymptotics of P_l; for the low multipoles of interest, $L\ll l$, the integral in Eq. (27) can be approximated by $[2/(2l'+1)\delta_{ll'}]$. After performing the Matsubara summation, for the imaginary part of the self-energy that determines the electron scattering rate we obtain

$$\mathrm{Im}\,\Sigma^c_\alpha(\omega)=-\frac{16e^2}{R}E_0^2\sum_L L^2\times\int dEg_l(E)\frac{EE^c_\alpha}{(E^c_\alpha-E)^4}\mathrm{Im}\frac{N(E-\omega)+f(E)}{\tilde{\epsilon}_L(E-\omega)}, \tag{28}$$

where $N(E)$ is the Bose distribution and $g_l(E)$ is the density of states of a conduction electron with angular momentum l,

$$g_l(E)=2\sum_n\delta(E^c_{nl}-E)\simeq\frac{R}{\pi}\sqrt{\frac{2m}{E}}, \tag{29}$$

where we replaced the sum over n by an integral (the factor of 2 accounts for spin).

Each term in the sum on the right-hand side of Eq. (28) represents a channel of electron scattering mediated by a collective surface mode with angular momentum L. For low L, the difference between the energies of modes with successive values of L is larger than their widths, so the different channels are well separated. Note that since all ω_L are smaller than the frequency of the bulk plasmon, one can replace $\tilde{\epsilon}_L(\omega)$ by $\epsilon_L(\omega)$ in the integrand of Eq. (28) for frequencies $\omega\sim\omega_L$.

Consider now the $L=1$ term in Eq. (28), which describes the SP-mediated scattering channel. The main contribution to the integral comes from the SP pole in $\epsilon_1^{-1}(\omega)=3\epsilon_s^{-1}(\omega)$, where $\epsilon_s(\omega)$ is the same as in Eq. (3). To evaluate the integral in Eq. (28), we can in the first approximation replace $\mathrm{Im}\,\epsilon_s^{-1}(\omega)$ by a Lorentzian,

$$\mathrm{Im}\frac{1}{\epsilon_s(\omega)}=-\frac{\gamma_s\omega_p^2/\omega^3+\epsilon_d''(\omega)}{[\epsilon'(\omega)+2\epsilon_m]^2+[\gamma_s\omega_p^2/\omega^3+\epsilon_d''(\omega)]^2}\simeq-\frac{\omega_s^2}{\epsilon_d'(\omega_s)+2\epsilon_m}\frac{\omega_s\gamma}{(\omega^2-\omega_s^2)^2+\omega_s^2\gamma^2}, \tag{30}$$

where $\omega_s\equiv\omega_1=\omega_p/\sqrt{\epsilon_d'(\omega_s)+2\epsilon_m}$ and $\gamma=\gamma_s+\omega_s\epsilon_d''(\omega_s)$ are the SP frequency and width, respectively. For typical widths $\gamma\ll\omega_s$, the integral in Eq. (28) can be easily evaluated, yielding

$$\mathrm{Im}\,\Sigma^c_\alpha(\omega)=-\frac{24e^2\omega_sE_0^2}{\epsilon_d'(\omega_s)+2\epsilon_m}\frac{E^c_\alpha\sqrt{2m(\omega-\omega_s)}}{(\omega-E^c_\alpha-\omega_s)^4}\times[1-f(\omega-\omega_s)]. \tag{31}$$

Finally, using the relation $e^2k_F[\epsilon_d'(\omega_s)+2\epsilon_m]^{-1}=3\pi\omega_s^2/8E_F$, the SP-mediated scattering rate, $\gamma^s_e(E^c_\alpha)=-\mathrm{Im}\,\Sigma^c_\alpha(E^c_\alpha)$, takes the form

$$\gamma^s_e(E)=9\pi\frac{E_0^2}{\omega_s}\frac{E}{E_F}\left(\frac{E-\omega_s}{E_F}\right)^{1/2}[1-f(E-\omega_s)]. \tag{32}$$

Recalling that $E_0=(2mR^2)^{-1}$, we see that the scattering rate of a conduction electron is *size dependent*: $\gamma^s_e\propto R^{-4}$. At $E=E_F+\omega_s$, the scattering rate jumps to the value $9\pi(1+\omega_s/E_F)E_0^2/\omega_s$, and then *increases* with energy as $E^{3/2}$ (for $\omega_s\ll E_F$). This should be contrasted with the usual (bulk) plasmon-mediated scattering, originating from the first term in Eq. (22), in which case the rate decreases as $E^{-1/2}$ above the onset.[27]

Note that the total electron scattering rate is the sum, $\gamma_e+\gamma^s_e$, of the SP-mediated (γ^s_e) and bulklike (γ_e) scattering rates. In order to be observable, the former should exceed the latter. The typical size at which γ^s_e becomes important can be estimated by equating γ^s_e and the Fermi-liquid e-e scattering rate,[24] $\gamma_e(E)=(\pi^2q_{\mathrm{TF}}/16k_F)[(E-E_F)^2/E_F]$. For energies $E\sim E_F+\omega_s$, the two rates become comparable for

$$(k_FR)^2\simeq12\frac{E_F}{\omega_s}\left(1+\frac{E_F}{\omega_s}\right)^{1/2}\left(\frac{k_F}{\pi q_{\mathrm{TF}}}\right)^{1/2}. \tag{33}$$

In the case of a Cu nanoparticle with $\omega_s\simeq2.2$ eV, we obtain $k_FR\simeq8$, which corresponds to a radius of $R\simeq3$ nm. At the same time, in this energy range, the width γ^s_e exceeds the mean level spacing δ, so that the energy spectrum is still continuous. The strong size dependence of γ^s_e indicates that, although γ^s_e increases with energy more slowly than γ_e, the SP-mediated scattering should dominate for nanometer-sized particles. Note also that the size and energy dependences of the scattering in the different channels are similar: the rate of scattering via the Lth channel is given by Eq. (32), with ω_s replaced by ω_L [Eq. (19)], and the numerical factor 9 replaced by $3L(2L+1)$.

Concluding this subsection, we have shown that the SP-mediated scattering is the dominant scattering mechanism of

conduction electrons in nanometer-sized nanoparticles for energies larger than ω_s but smaller than ω_p. The scattering rate in the Lth channel, γ_e^L, increases with energy, in sharp contrast with the bulk-plasmon-mediated scattering rate. The total scattering rate as a function of energy represents a series of steps at $E=\omega_L$, on top of a smooth energy increase. We expect that this effect should be observable experimentally by measuring *e-e* scattering rate in size-selected cluster beams in time-resolved two-photon photoemission spectrum.[29]

B. *d*-band hole scattering

We now turn to the interband processes in noble-metal particles and consider the scattering of a *d* hole into the conduction band. The corresponding surface-induced potential, given by the Lth term in Eq. (22), has the form

$$U_{LM}(\omega;\mathbf{r},\mathbf{r}')=\frac{4\pi}{2L+1}\frac{1}{\epsilon_L(\omega)}\frac{e^2}{R}\left(\frac{rr'}{R^2}\right)^L Y_{LM}(\hat{\mathbf{r}})Y^*_{LM}(\hat{\mathbf{r}}'), \tag{34}$$

where $\epsilon_L(\omega)$ is given by Eq. (18). With this potential, the *d*-hole self-energy is given by

$$\Sigma^d_\alpha(i\omega)=-\frac{e^2}{R^{2L+1}}\sum_{\alpha'}|\tilde{M}^{LM}_{\alpha\alpha'}|^2\frac{1}{\beta}\sum_{i\omega'}\frac{G^c_{\alpha'}(i\omega'+i\omega)}{\epsilon_L(i\omega')}, \tag{35}$$

where $\tilde{M}^{LM}_{\alpha\alpha'}=\langle c,\alpha|r^L Y_{LM}(\hat{\mathbf{r}})|d,\alpha'\rangle$ is the *interband* transition matrix element [compare with Eq. (24)]. Since the final-state energies in the conduction band are high (in the case of interest here, they are close to the Fermi level), the matrix element can be approximated by a bulklike expression $\tilde{M}^{LM}_{\alpha\alpha'}=\delta_{\alpha\alpha'}\tilde{M}^{LM}_{\alpha\alpha}$, the corrections due to surface scattering being suppressed by a factor of $(k_FR)^{-1}\ll 1$.

The largest contribution to the self-energy [Eq. (35)] comes from the dipole channel $L=1$, mediated by the SP. In this case, after performing the frequency summation, for $\mathrm{Im}\,\Sigma^d_\alpha$ we obtain

$$\mathrm{Im}\,\Sigma^d_\alpha(\omega)=-\frac{9e^2\mu^2}{m^2(E^{cd}_\alpha)^2R^3}\mathrm{Im}\frac{N(E^c_\alpha-\omega)+f(E^c_\alpha)}{\epsilon_s(E^c_\alpha-\omega)}, \tag{36}$$

where $E^{cd}_\alpha=E^c_\alpha-E^d_\alpha$ and μ is the interband dipole matrix element.[17] We see that the scattering rate of a *d* hole with energy E^d_α, $\gamma^s_h(E^d_\alpha)=\mathrm{Im}\,\Sigma^d_\alpha(E^d_\alpha)$, has a strong R^{-3} dependence on the nanoparticle size, which is, however, different from that of the intraband scattering [Eq. (32)].

The most important difference between the interband and intraband SP-mediated scattering rates, derived in Sec. III, lies in their dependence on energy. Since the surface-induced potential [Eq. (34)], only allows for vertical (dipole) interband single-particle excitations, the phase space available for the scattering of a *d* hole with energy E^d_α is restricted to a *single* final state in the conduction band, with energy E^c_α. As a result of this restriction, the *d*-hole scattering rate $\gamma^s_h(E^d_\alpha)$ exhibits a *peak* as the difference between the energies of final and initial states, $E^{cd}_\alpha=E^c_\alpha-E^d_\alpha$, approaches the SP frequency ω_s [see Eq. (36)]. In contrast, the energy dependence of γ^s_e is smooth due the larger phase space available for scattering within the conduction band. This leads to the additional integral over final-state energies in Eq. (28), which smears out the SP resonant enhancement of the intraband scattering.

As we show in Sec. IV, the fact that the scattering rate of a *d* hole is dominated by the SP resonance strongly affects the nonlinear optical dynamics in small nanoparticles. This is the case, in particular, when the SP frequency ω_s is close to the onset of interband transitions Δ, as, e.g., in Cu and Au nanoparticles.[1,12,14,16] Indeed, if the optical pulse excites an *e-h* pair with excitation energy ω close to Δ, the *d* hole can subsequently scatter into the conduction band by emitting a SP. According to Eq. (36) for $\omega\sim\omega_s$, such a scattering process should be resonantly enhanced. In order to have an observable effect on the absorption spectrum, the scattering rate of the photoexcited *d* hole should be comparable (or larger than) that of the photoexcited electron. Close to E_F the electron scattering in the conduction band comes from a two-quasiparticle process; the corresponding rate in noble metals is estimated as[29] $\gamma_e\sim 10^{-2}$ eV. If one assumes the bulk value for $\mu(2\mu^2/m\sim 1$ eV near the L-point[30]), then γ^s_h exceeds γ_e for $R\lesssim 2.5$ nm. In fact, one would expect that, in nanoparticles, μ is larger than in the bulk due to the localization of the conduction electron wave functions.[1]

IV. SURFACE PLASMON NONLINEAR OPTICAL DYNAMICS

In this section, we study the effect of the SP-mediated *interband* scattering on the ultrafast optical dynamics in noble-metal nanoparticles. In particular, we study the *size dependence* of the differential absorption measured in the pump-probe spectroscopy.

We are interested in the situation when the hot electron distribution has already thermalized and the electron gas is cooling to the lattice. In this case the transient response of a nanoparticle can be described by the time-dependent absorption coefficient $\alpha(\omega,t)$, given by Eq. (2) with time-dependent temperature.[31] In noble-metal particles, the temperature dependence of α originates from two different sources. First is the phonon-induced correction to γ_s, which is proportional to the *lattice* temperature $T_l(t)$. As mentioned in Sec. I, for small nanoparticles this effect is relatively weak. Second, near the onset of the interband transitions, Δ, the absorption coefficient depends on the *electron* temperature $T(t)$ via the interband dielectric function $\epsilon_d(\omega)$ [see Eqs. (2) and (3)]. In fact, in Cu or Au nanoparticles, ω_s can be tuned close to Δ, so the SP damping by *interband e-h* excitations leads to an additional broadening of the absorption peak.[1] In this case, it is the temperature dependence of $\epsilon_d(\omega)$ that dominates the pump-probe dynamics. Below we show that, near the SP resonance, both the temperature and frequency dependence of $\epsilon_d(\omega)=1+4\pi\chi_d(\omega)$ are strongly affected by the SP-mediated interband scattering.

We start with the RPA expression for the interband susceptibility,[27] $\chi_d(i\omega)=\tilde{\chi}_d(i\omega)+\tilde{\chi}_d(-i\omega)$,

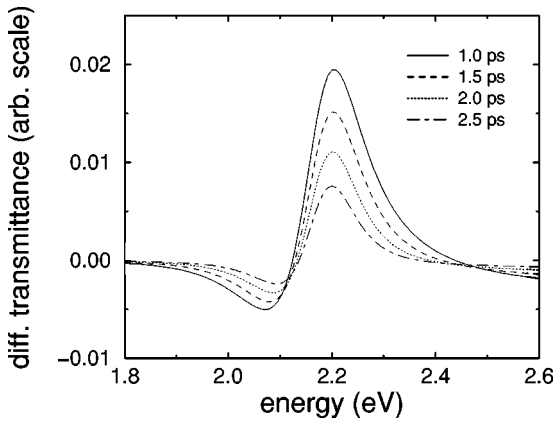

FIG. 1. Calculated differential transmission spectra at positive time delays for $R=5$ nm nanoparticles with initial electron temperature $T_0=1000$ K (other parameters are given in the text).

$$\tilde{\chi}_d(i\omega)=-\sum_\alpha \frac{e^2\mu^2}{m^2(E_\alpha^{cd})^2}\frac{1}{\beta}\sum_{i\omega'} G_\alpha^d(i\omega')G_\alpha^c(i\omega'+i\omega), \tag{37}$$

where $G_\alpha^d(i\omega')$ is the Green function of a d electron. With the d band fully occupied, the only allowed SP-mediated interband scattering is that of the d hole. We assume here, for simplicity, a dispersionless d band with energy E^d. Substituting $G_\alpha^d(i\omega')=[i\omega'-E^d+E_F-\Sigma_\alpha^d(i\omega')]^{-1}$, with $\Sigma_\alpha^d(i\omega)$ given by Eq. (35), and performing the frequency summation, we obtain

$$\tilde{\chi}_d(\omega)=\frac{e^2\mu^2}{m^2}\int \frac{dE^c g(E^c)}{(E^{cd})^2}\frac{f(E^c)-1}{\omega-E^{cd}+i\gamma_h^s(\omega,E^c)}, \tag{38}$$

where $g(E^c)$ is the density of states of conduction electrons. The scattering rate of a d hole, $\gamma_h^s(\omega,E^c)=\mathrm{Im}\,\Sigma^d(E^c-\omega)$, is obtained from Eq. (36) with $E_d=E^c-\omega$:

$$\gamma_h^s(\omega,E^c)=-\frac{9e^2\mu^2}{m^2(E^{cd})^2R^3}f(E^c)\,\mathrm{Im}\frac{1}{\epsilon_s(\omega)}, \tag{39}$$

where $N(\omega)$ is negligible for frequencies $\omega\sim\omega_s\gg k_BT$.[17] The rate $\gamma_h^s(\omega,E^c)$ exhibits a sharp peak as a function of the frequency of the probe optical field. The reason for this is that the scattering rate of a d hole with energy E depends explicitly on the *difference* between the final and initial states, E^c-E, as discussed in Sec. III; therefore, for a d hole with energy $E=E^c-\omega$, the dependence on the final-state energy, E^c, cancels out in $\epsilon_s(E^c-E)$ [see Eq. (36)]. In other words, the optically excited d hole scatters resonantly into the conduction band as ω approaches ω_s. It is important to note that $\gamma_h^s(\omega,E^c)$ is, in fact, proportional to the absorption coefficient $\alpha(\omega)$ [see Eq. (2)]. Therefore, α and γ_h^s should be calculated self-consistently from Eqs. (2), (3), (38), and (39).

It should be emphasized that the effect of γ_h^s on $\epsilon_d''(\omega)$ increases with temperature. Indeed, it can be seen from Eq. (39) that the value of γ_h^s is appreciable only if $E^c-E_F\gtrsim k_BT$. Since the main contribution to $\tilde{\chi}_d''(\omega)$ comes from energies $E^c\sim\omega-\Delta+E_F$, the effect of d hole scattering on the absorption becomes important only for elevated electron temperatures: $k_BT\gtrsim\omega_s-\Delta$. As a result, near the SP resonance, the time evolution of the differential absorption, which is governed by the temperature dependence of α, becomes strongly *size dependent*, as we show in the rest of this section.

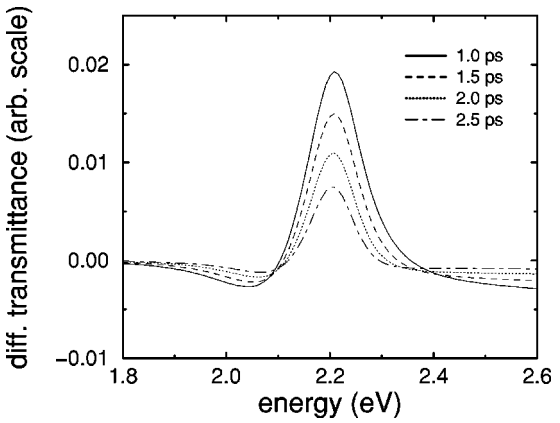

FIG. 2. Calculated differential transmission spectra for $R=2.5$ nm nanoparticles.

In the numerical calculations below, we adopt the parameters of Ref. 12, where pump-probe measurements on $R\simeq 2.5$ nm Cu nanoparticles were performed. In this experiment, the SP frequency $\omega_s\simeq 2.22$ eV was slightly above the onset of the interband transitions, $\Delta\simeq 2.18$ eV. In order to describe the time evolution of the differential absorption spectra, we first need to determine the time dependence of the electron temperature, $T(t)$, due to the relaxation of the electron gas to the lattice. For this, we employ a simple two-temperature model, defined by heat equations for $T(t)$ and the lattice temperature $T_l(t)$:

$$C(T)\frac{\partial T}{\partial t}=-G(T-T_l),\quad C_l\frac{\partial T_l}{\partial t}=G(T-T_l), \tag{40}$$

where $C(T)=\Gamma T$ and C_l are the electron and lattice heat capacities, respectively, and G is the electron-phonon coupling.[32] The parameter values used here were $G=3.5\times 10^{16}$ W m^{-3}K^{-1}, $\Gamma=70$ J m^{-3}K^{-2}, and $C_l=3.5$ J m^{-3}K^{-1}, and the initial condition was taken as $T_0=1000$ K. We then self-consistently calculated the time-dependent absorption coefficient $\alpha(\omega,t)$, and the differential

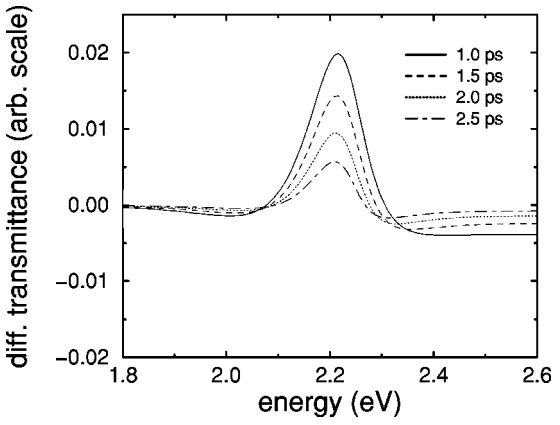

FIG. 3. Calculated differential transmission spectra for $R=1.8$ nm nanoparticles.

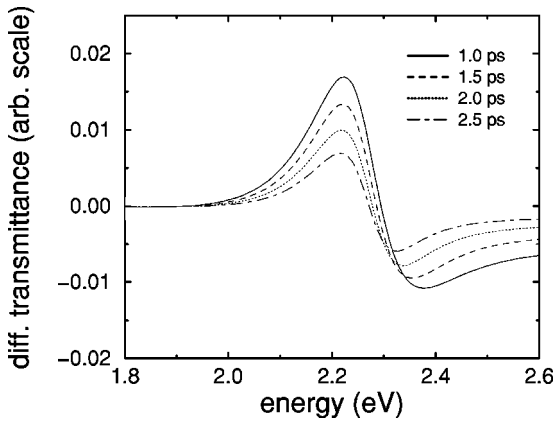

FIG. 4. Calculated differential transmission spectra at positive time delays for $R=1.2$ nm nanoparticles.

transmission is proportional to $\alpha_r(\omega)-\alpha(\omega,t)$, where $\alpha_r(\omega)$ was calculated at room temperature.

We now study the size dependence of the optical dynamics originating from the SP-mediated *d*-hole scattering. In Figs. 1–4 we plot the calculated differential transmission spectra with decreasing nanoparticle size. Figure 1 shows the spectra at several time delays for $R=5.0$ nm; in this case, the SP-mediated *d*-hole scattering has no significant effect. Note that it is necessary to include the effect of the intraband *e-e* scattering in order to reproduce the differential transmission line shape observed in the experiment.[12] For optically excited electron energy close to E_F, this can be achieved by adding the *e-e* scattering rate[24] $\gamma_e(E^c)\propto[1-f(E^c)][(E^c-E_F)^2+(\pi k_B T)^2]$ to γ_h^s in Eq. (38). The difference in $\gamma_e(E^c)$ for E^c below and above E_F then leads to a line shape similar to that expected from the combination of redshift and broadening. Note, however, that $\gamma_e(E^c)$ is essentially bulklike, so that its effect on the absorption does not change with decreasing nanoparticle size.

Figure 2 shows the differential transmission spectra for $R=2.5$ nm. It can be seen that in this case the apparent redshift is *reduced*. This effect becomes more prominent for smaller sizes. It can be seen in Fig. 3 that with further decrease in *R*, the redshift gives way to the apparent *blueshift*,

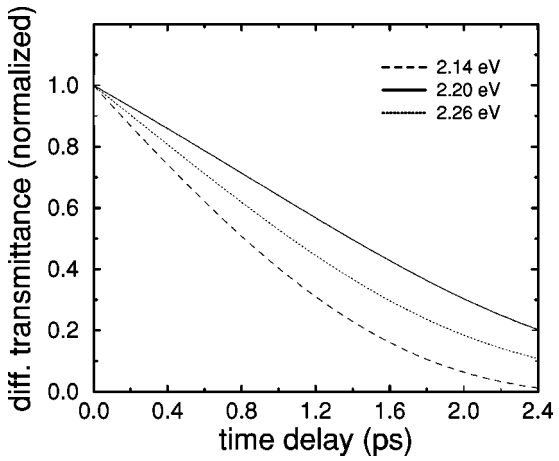

FIG. 5. Temporal evolution of the differential transmission at different frequencies close to the SP resonance for $R=5$ nm nanoparticles with $T_0=1000$ K (other parameters are given in the text).

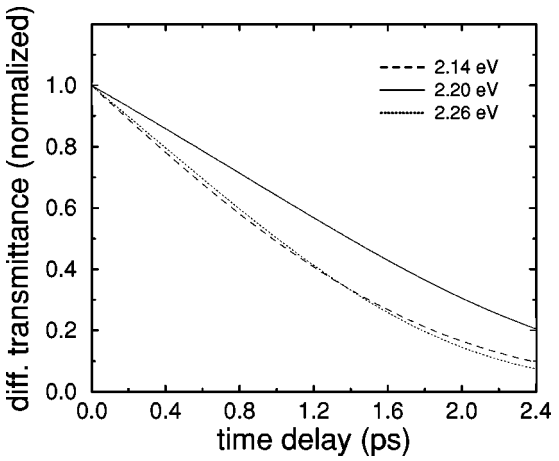

FIG. 6. Temporal evolution of the differential transmission for $R=2.5$ nm nanoparticles.

and for even smaller sizes the latter becomes the dominant feature of the spectrum [see Fig. 4)].

The above transition in the differential transmission line shape with decreasing size can be explained as follows. Since $\omega_s\sim\Delta$, the SP is damped by the interband excitations for $\omega>\omega_s$, so that the absorption peak is *asymmetric*. The *d*-hole scattering with the SP enhances this damping; since the ω dependence of γ_h^s follows that of α, this effect is larger above the resonance. On the other hand, the efficiency of the scattering increases with temperature, as discussed above. Therefore, for short time delays, the *d*-hole scattering leads to a relative increase in the absorption for $\omega>\omega_s$. This in turn transforms the apparent redshift into the blueshift for small nanoparticle sizes. Note that such a transition cannot be described within the RPA or with dielectric function of Ref. 12, in which case the change in the differential transmission line shape is mainly determined by the linear absorption spectrum.

Let us now turn to the time evolution of the differential transmission. An important feature of the measured pump-probe signal is that its relaxation depends on the probe frequency.[12] In Figs. 5–8 we show the time evolution of the differential transmission at several different frequencies close to ω_s. It can be seen that, for all sizes, the relaxation is

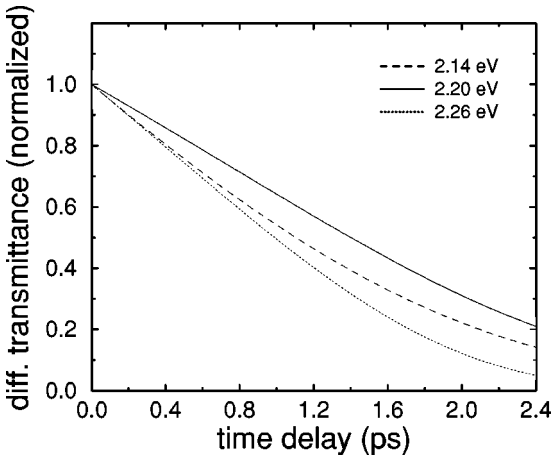

FIG. 7. Temporal evolution of the differential transmission for $R=1.8$ nm nanoparticles.

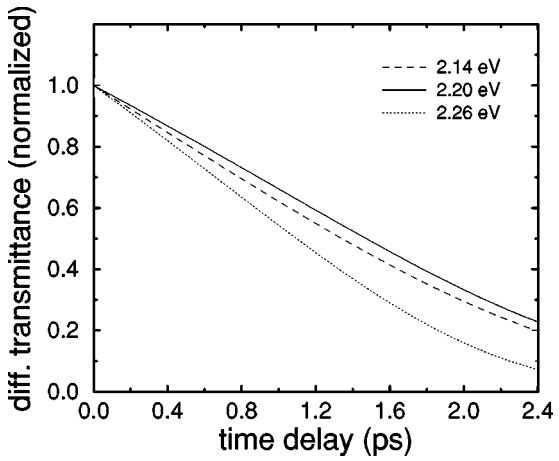

FIG. 8. Temporal evolution of the differential transmission for $R=1.2$ nm nanoparticles.

slowest at the SP resonance; this characterizes the robustness of the collective mode, which determines the peak position, versus the single-particle excitations, which determine the resonance width. For larger sizes, at which γ_h^s is negligible, the change in the differential transmission decay rate with *frequency* is slower above the resonance [see Fig. 2(a)]. This stems from the asymmetric line shape of the absorption peak, mentioned above: the absorption is larger for $\omega>\omega_s$, so that its *relative* change with temperature is weaker. For a smaller nanoparticle size, at which the SP-mediated *d*-hole scattering becomes relevant, the decay rates become similar above and below ω_s (see Fig. 6). This change in the frequency dependence is related to the stronger SP damping for $\omega>\omega_s$ due to the *d*-hole scattering, as discussed above. Since this additional damping is reduced with decreasing temperature, the relaxation is faster above the resonance, despite the relatively weaker change in the absorption. This rather ''nonlinear'' relation between the time evolution of the pump-probe signal and that of the temperature, becomes even stronger for smaller sizes (see Figs. 7 and 8). In this case, the frequency dependence of the differential transmission decay below and above ω_s is reversed. Note that a frequency dependence consistent with our calculations presented in Fig. 6 was, in fact, observed in the pump-probe experiment.[12,17] At the same time, the effects of this mechanism on the linear absorption spectrum are relatively small.

Thus the correlations between the optically excited collective and single-particle excitations (SP and *d* hole) profoundly change the optical dynamics at smaller sizes. The reason for this is the resonant dependence of the *d*-hole scattering rate on the optical probe frequency. The above strong size dependence of the differential transmission originates from the R^{-3} dependence of the *d*-hole SP-mediated scattering rate; reducing the size by a factor of 2 results in an enhancement of γ_h^s by an order of magnitude.

V. CONCLUSIONS

In summary, we have theoretically examined the role of size-dependent correlations in electron relaxation in small metal particles. We identified a mechanism of quasiparticle scattering, mediated by collective surface excitations, which originates from the surface-induced dynamical screening of the *e*-*e* interactions. The behavior of the corresponding scattering rates with varying energy and temperature differs substantially from that in the bulk metal. We have shown that the conduction electron scattering rate increases with energy, in sharp contrast to the bulk behavior, which could be observed in two-photon photoemission measurements. We also found that in noble-metal particles, the resonant energy dependence of the *d*-hole scattering rate affects strongly the differential absorption.

An important aspect of the SP-mediated scattering is its strong dependence on size. Our estimates show that it becomes comparable to the usual Fermi-liquid scattering in nanometer-sized particles. This size regime is, in fact, intermediate between ''classical'' particles with sizes larger than 10 nm, where the bulklike behavior dominates, and very small clusters with only dozens of atoms, where the metallic properties are completely lost. Although the static properties of nanometer-sized particles are also size dependent, the deviations from their bulk values do not change the qualitative features of the electron *dynamics*. In contrast, the size-dependent *many-body* effects, studied here, *do* affect the dynamics in a significant way during time scales comparable to the relaxation times. As we have shown, the SP-mediated interband scattering reveals itself in the size dependence of the transient pump-probe spectra. In particular, as the nanoparticle size decreases, the calculated time-resolved differential absorption line shape shows a transition from an apparent redshift to a blueshift. This transition, absent in the RPA, comes from the correlations between collective surface and single-particle excitations. At the same time, near the SP resonance, this correlation leads to significant size-dependent changes in the frequency dependence of the relaxation time of the pump-probe signal. These results indicate the need for systematic experimental studies of the size dependence of the transient nonlinear optical response, as we approach the transition from boundary-constrained nanoparticles to molecular clusters.

ACKNOWLEDGMENTS

The authors thank J.-Y. Bigot for valuable discussions. This work was supported by NSF Grant No. ECS-9703453, and, in part, by ONR Grant No. N00014-96-1-1042 and by ARL, Hitachi Ltd.

[1] See, e.g., U. Kreibig and M. Vollmer, *Optical Properties of Metal Clusters* (Springer, Berlin, 1995), and references therein.

[2] See, e.g., W.A. De Heer, Rev. Mod. Phys. **65**, 611 (1993).

[3] See, e.g., M. Brack, Rev. Mod. Phys. **65**, 677 (1993).

[4] See, e.g., *Physics and Chemistry of Finite Systems: From Clusters to Crystals*, edited by P. Jena, S. N. Khanna, and B. K. Rao, Vol. 374 of *NATO Advanced Study Institute, Series C: Mathematical and Physical Sciences* (Kluwer, Dordrecht, 1992).

[5] C. Flytzanis, F. Hache, M.C. Klein, D. Ricard, and Ph. Roussignol, in *Progress in Optics XXIX*, edited by E. Wolf (Elsevier, Amsterdam, 1991), p. 321.
[6] A. Kawabata and R. Kubo, J. Phys. Soc. Jpn. **21**, 1765 (1966).
[7] F. Hache, D. Ricard, and C. Flytzanis, J. Opt. Soc. Am. B **3**, 1647 (1986).
[8] G.S. Agarwal and S.D. Gupta, Phys. Rev. A **38**, 5678 (1988).
[9] L. Yang, K. Becker, F.M. Smith, R.H. Magruder, R.F. Haglund, L. Yang, R. Dorsinville, R.R. Alfano, and R.A. Zuhr, J. Opt. Soc. Am. B **11**, 457 (1994).
[10] T. Tokizaki, A. Nakamura, S. Kaneko, K. Uchida, S. Omi, H. Tanji, and Y. Asahara, Appl. Phys. Lett. **65**, 941 (1994).
[11] T.W. Roberti, B.A. Smith, and J.Z. Zhang, J. Chem. Phys. **102**, 3860 (1995).
[12] J.-Y. Bigot, J.-C. Merle, O. Cregut, and A. Daunois, Phys. Rev. Lett. **75**, 4702 (1995).
[13] T.S. Ahmadi, S.L. Logunov, and M.A. Elsayed, J. Phys. Chem. **100**, 8053 (1996).
[14] M. Perner, P. Bost, G. von Plessen, J. Feldmann, U. Becker, M. Mennig, M. Schmitt, and H. Schmidt, Phys. Rev. Lett. **78**, 2192 (1997).
[15] M. Nisoli, S. Stragira, S. De Silvestri, A. Stella, P. Tognini, P. Cheyssac, and R. Kofman, Phys. Rev. Lett. **78**, 3575 (1997).
[16] T. Klar, M. Perner, S. Grosse, G. von Plessen, W. Spirkl, and J. Feldmann, Phys. Rev. Lett. **80**, 4249 (1998).
[17] T.V. Shahbazyan, I.E. Perakis, and J.-Y. Bigot, Phys. Rev. Lett. **81**, 3120 (1998).
[18] W.S. Fann, R. Storz, and H.W.K. Tom, Phys. Rev. B **46**, 13 592 (1992).
[19] C.K. Sun, F. Vallée, L.H. Acioli, E.P. Ippen, and J.G. Fujimoto, Phys. Rev. B **50**, 15 337 (1994).
[20] R.H.M. Groeneveld, R. Sprik, and A. Lagendijk, Phys. Rev. B **51**, 11 433 (1994).
[21] N. Del Fatti, R. Bouffanais, F. Vallée, and C. Flytzanis, Phys. Rev. Lett. **81**, 922 (1998).
[22] The effects of the spillout of the electron wave functions beyond the nanoparticle classical boundary were discussed, e.g., by V.V. Krezin, Phys. Rep. **220**, 1 (1992).
[23] U. Sivan, Y. Imry, and A.G. Aronov, Europhys. Lett. **28**, 115 (1994).
[24] D. Pines and P. Nozieres, *The Theory of Quantum Liquids* (Benjamin, New York, 1966), Vol. I.
[25] In semiconductor quantum dots, where the discrete energy levels are well resolved, the quasiparticle scattering rate is similar to that in the bulk only for energies larger than some critical energy; see, e.g., B.I. Altshuler, Y. Gefen, A. Kamenev, and L.S. Levitov, Phys. Rev. Lett. **78**, 2803 (1997).
[26] A.A. Lushnikov and A.J. Simonov, Z. Phys. **270**, 17 (1974).
[27] See, e.g., G.D. Mahan, *Many-Particle Physics* (Plenum, New York, 1990).
[28] In very small particles, the difference in the positions of the effective boundaries for the conduction and *d*-band densities leads to a shift in the linear absorption peak; see A. Liebsch, Phys. Rev. B **48**, 11 317 (1993); V.V. Krezin, *ibid.* **51**, 1844 (1995).
[29] S. Ogawa, H. Nagano, and H. Petek, Phys. Rev. B **55**, 10 869 (1997).
[30] H. Ehrenreich and H.R. Philipp, Phys. Rev. **128**, 1622 (1962).
[31] The notion of a time-dependent absorption coefficient can also be extended to the coherent regime; see I.E. Perakis, Chem. Phys. **210**, 259 (1996); I.E. Perakis, I. Brener, W.H. Knox, and D.S. Chemla, J. Opt. Soc. Am. B **13**, 1313 (1996); I.E. Perakis and D.S. Chemla, Phys. Rev. Lett. **72**, 3202 (1994).
[32] G.L. Easley, Phys. Rev. B **33**, 2144 (1986).